硅表面含二茂铁基团自组装单分子膜制备及电流-电压关系测量

裴 佳[1] 夏 兵*,[1,2] 晁 洁[1] 王海涛[2] 刘洪波[1] 肖忠党[2] 肖守军*,[1]
([1]南京大学配位化学国家重点实验室,南京 210093)
([2]东南大学生物电子学国家重点实验室,南京 210096)

摘要: 合成了一种头基为二茂铁基团的长链烯烃分子(Fc-CO-NH-$(CH_2)_9$-CH=CH_2) (FcUA),并用红外、核磁、质谱等手段对其进行了表征。用微波引发将该化合物嫁接到平面硅的表面,并用 X 射线光电子能谱、反射红外光谱、原子力显微镜表征了这一过程。最后,通过循环伏安电化学法和电敏感原子力显微镜的导电模式对其进行电学性质测试。结果表明这层单分子膜可以提高硅片的介电常数。同时还观察到了一种不稳定的类似负微分电流现象。

关键词: 硅; 单分子膜; 二茂铁; 电子传递
中图分类号: O613.72; O649.2 **文献标识码**: A **文章编号**: 1001-4861(2007)09-1505-10

Ferrocenyl Self-assembled Monolayer on Silicon Surfaces: Preparation and Current-Voltage Measurement

PEI Jia[1] XIA Bing*,[1,2] CHAO Jie[1] WANG Hai-Tao[2] LIU Hong-Bo[1] XIAO Zhong-Dang[2] XIAO Shou-Jun*,[1]
([1]*State Key Laboratory of Coordination Chemistry, Nanjing University, Nanjing* 210093)
([2]*State Key Laboratory of Molecular and Biomolecular Electronics, Southeast University, Nanjing* 210096)

Abstract: An electroactive compound of ferrocene monocarboxylic acid *N*-10-undecenamide (Fc-CO-NH-$(CH_2)_9$-CH=CH_2) (FcUA) was synthesized and then attached on H-terminated Si(100) surface by microwave irradiation. The monolayer was characterized by X-ray photoelectron spectroscopy (XPS), atomic force microscopy (AFM), infrared spectroscopy (IR) and cyclic voltammograms (CV) measurements. Current-voltage measurements at room temperature were carried out through the ferrocene-terminated monolayer by current sensing atomic force microscopy (CSAFM). The results reveal that the ferrocenyl monolayer improves the dielectric strength of the Metal(Pt)/Insulator(FcUA)/Metal(Si) structure. And NDR (negative differential resistance)-like peaks at the positive bias were also observed no matter it is n- or p-type of silicon.

Key words: silicon; monolayers; ferrocene; electron transfer

A redox monolayer based molecular junction has been studied since 2000[1,2], which shows that electron transfer could be tuned between the substrate and molecules. Considering the integration of a molecular junction with the well-established silicon micro-fabrication technology, it is necessary to study the molecular monolayers assembled on silicon and their electrical properties[3~12]. And these studies would offer opportunities for new applications in information processing, electron transport, and antistiction coatings for novel silicon-based nanoelectronic devices. The redox molecules containing ferrocene (Fc) species

收稿日期:2007-05-08。收修改稿日期:2007-08-22。
自然科学基金项目(No.20571042)和江苏省青蓝工程项目资助。
*通讯联系人。E-mail:nj_xiabing@yahoo.com.cn;sjxiao@nju.edu.cn
第一作者:裴 佳,女,25 岁,硕士生;研究方向:表面化学。

have been proposed as suitable electroactive moieties anchored on metal substrates, mainly in view of their well-known advantages in terms of chemical and thermal stability, robustness, reversible cyclability of the $Fc^{II} \rightleftharpoons Fc^{III}$ redox couple, wide synthetic availability of substituted Fc analogues, and tunability of the corresponding redox potential. Some molecules containing Fc species had been attached on silicon by Si-O-R bond, such as 1,1′-ferrocenyldichlorosilane, ferrocenemethanol, *N*,*N*-dimethylaminomethylferrocene, ferrocenylphosphine, and 4-(hydroxymethyl)phenylferrocene[13~16]. Especially the electron transfer and charge storage of 4-(hydroxymethyl)phenylferrocene was suggested by Lindsey's group as a potential alternative for computer random access memory[16]. But the Si-O-R linker is easily hydrolysable. In particular, silanisation is difficult to prevent the deposition of multilayers, thus always resulting in a polymer film. However, the superior Si-C bonded monolayers are relatively robust and possess a long-term stability towards the aqueous hydrolysis[17,18]. Recently a commercially available molecule (vinylferroence) attached on silicon surface by the Si-C bond has been studied[19~21]. The electron transfer through the Si-C bond was shown to be faster than the Si-O-C bond because of the presence of silicon oxide. The Si-C bond would be more suitable than Si-O-C for the silicon-based nanoelectronic devices. But more information about the electrical properties such as current-voltage relationship is still not rich enough for application in nanoelectronic devices. In addition, an interesting NDR phenomenon has been observed for the Fc-terminated monolayer on gold, indicating tuning of the electron transfer by the Fc moiety[22~25]. If the similar phenomenon presents on the silicon surface, the molecular junction would integrate with microelectronics and probably implement logical operations and refresh random access memory cells.

In our work, we synthesized a Fc-containing molecule, FcUA, then covalently attached it on hydrogen-terminated silicon. The CSAFM was used to study the electrical behavior of the monolayer in nano-sized regions[26~29]. The aspects of CSAFM that are most attractive for nanoscale electrical transport measurements are (1) the ability to image samples with high resolution before, during, and after the measurement, (2) the ability to record current-voltage relationships on samples that are highly resistive or are surrounded by insulating regions, and (3) straightforward interpretation of the tip position relative to the sample (*i.e.* a measured repulsive force indicates intimate tip-sample contact), where the contact force is known and controlled unlike STM. During the experiment, we studied the electric character of different doped types of silicon after grafting FcUA. The dielectric strength of the Pt/FcUA/Si junction was improved with regarding to the junction Pt/Si-H. No matter it was n-Si or p-Si, there were NDR-like peaks at the positive bias after the FcUA attachment. But the mechanism of these peaks is still under argument. For the Fc-terminated monolayer on gold, the NDR effect was mostly described by one-step resonant tunneling [22,23,30~32] or two-step reduction/oxidation [24,33,34]. Recently Lindsay et al. proposed a new mechanism of irreversible redox of Fc, which arised as a consequence of chemical changes in the material [25]. For styrene attached on silicon, Hersam et al. thought the NDR effect was due to resonant tunneling[35,36], consistent with the theory proposed by Datta et al.[37~39] But Wolkow et al. thought the NDR effect was attributed to the molecular rearrangement, desorption and decomposition with increasing frequency at a large voltage and current settings[40]. Here our experimental phenomena further proved Wolkow's interpretation of the FcUA rearrangement, oxidation, desorption, and decomposition, which is helpful for its application integrated with microelectronics in logical operations and refresh random access memory cells.

1 Experimental

1.1 Materials

Silicon wafers were purchased from Huajing Microelectronics Co., Ltd (Wuxi, China). 10-Undencenoic acid (UA) (Purity: ≥99%) was purchased from Sigma-Aldrich, diisopropylethylamine (DIEA) (Purity: ≥98%) from Acros Organics, and ammonium hydroxide (25%, *w*/*w*), chloroform (CA), methanol (CA), ethyl acetate (CA), petroleum ether (CA) were purchased

from Sinopharm Chemical Reagent Co., Ltd and used as received without further purification.

1.2 Synthesis of 10-Undecenamide

10-Undecenamide was prepared by refluxing UA with an excess of thionyl chloride for 1 h. After removal of excess thionyl chloride under reduced pressure the crude 10-undecenoic acid chloride was added dropwise to a vigorously stirring ice-cold solution of ammonium hydroxide (25%, *w*/*w*). The cream colored precipitate was filtered off by suction to yield crude 10-undecenamide. The product was purified by flash chromatography (silica gel: 2.5×30 cm, eluent: chloroform/methanol, 9/5(*V*/*V*)) to afford a colorless solid (30 mg, yield 82.1%)[41].

1.3 Synthesis of 10-Undecenamine

The amine was prepared by reduction of the amide with $LiAlH_4$. A solution of 10-undecenamide (6.0 g, 32.7 mmol) in 115 mL anhydrous tetrahydrofuran was slowly added with a dropping funnel to a stirring and gently refluxing suspension of $LiAlH_4$ (2.9 g, 75.6 mmol) in 58 mL anhydrous tetrahydrofuran. The reaction solution was refluxed under a nitrogen atmosphere for 15 h. The mixture was chilled on an ice-bath and water (10 mL) was added dropwise to decompose excess $LiAlH_4$. The resulting grey-white precipitate was removed by filtration and washed three times with ethyl acetate. The combined organic phase was dried over Na_2SO_4 and evaporated under reduced pressure to yield 10-undecenamine as oil. The product was purified by flash chromatography (silica gel: 2.5×30 cm, eluent: chloroform/methanol/water, 65/40/9 (*V*/*V*)) to afford a light brown oil (2.8 g, yield 90%). ^{1}H NMR (500 MHz, $CDCl_3$): δ (ppm) 5.85~5.79 (1H, m, -CH_2=CH-), 5.01~4.92 (2H, m, -CH_2=CH-), 2.70~2.68 (2H, t, -CH_2-NH_2), 2.06~2.03 (2H, m, =CH-CH_2-), 1.45 (2H, q, -CH_2-CH_2-NH_2), 1.42~1.35 (2H, m, =CH-CH_2-CH_2-), 1.29 (10H, bs, (-CH_2-)$_5$)[41].

1.4 Synthesis of ferrocene monocarboxylic acid *N*-hydroxysuccinimide ester (FcSu)

Ferrocenecarboxylic acid (5.5 g, 24.0 mmol) was dissolved in CH_2Cl_2 (100 mL), and solid dicyclohexylcarbodiimide (DCC) (5.0 g, 24.0 mmol) and *N*-hydroxysuccinimide (2.4 g, 24.0 mmol) were added. After 3 h stirring at room temperature, DCC was removed by filtration. The filtrate was washed with saturated $NaHCO_3$ solution (500 mL), followed by distilled water (500 mL), and then dried over $MgSO_4$. The solvent was removed in vacuo. The product was purified by flash chromatography (silica gel: 2.5×30 cm, eluent: petroleum ether (60~90 ℃) /ethyl acetate, 5/3 (*V*/*V*)) to afford a dark red crystalline product (6.5 g, yield 83.8%). ^{1}H NMR (500 MHz, $CDCl_3$): δ (ppm) 4.96~4.95 (2H, s, H ortho to carboxy group on Cp ring), 4.58 (2H, s, H meta to carboxy group on Cp ring), 4.21 (5H, s, unsubstituted Cp ring), 2.90~2.88 (4H, t, H to succinimide). FTIR (KBr), ν(cm^{-1}): 3 115, 1 767, 1 736 and 1 378[42].

1.5 Synthesis of FcUA

A solution of FcSu (5.4 g, 16.5 mmol) dissolved in CH_2Cl_2 (165 mL) was added dropwise to a stirring solution of 10-undecenamine (2.8 g, 16.5 mmol) and DIEA (6.0 mL, 34.7 mmol) in CH_2Cl_2 (165 mL) under nitrogen. The reaction mixture was allowed stirring for 48 h at room temperature. After evaporation of volatiles under reduced pressure, the product was purified by flash chromatography (silica gel: 2.5×30 cm, eluent, petroleum ether (60~90 ℃)/ethyl acetate, 5:3 (*V*/*V*)) to afford a gold yellow sheet crystal (4.9 g, yield 37.1%). ^{1}H NMR (500 MHz, $CDCl_3$): δ (ppm) 5.94 (1H, s, -CH_2=-CH-), 5.73 (1H, s, -CH_2-NH-), 5.30~5.19 (2H, m, -CH_2=CH-), 4.72 (2H, s, H ortho to carboxy group on Cp ring), 4.39 (2H, s, H meta to carboxy group on Cp ring), 4.26 (5H, s, unsubstituted Cp ring), 4.03 (2H, s, -CH_2-NH-). FTIR (KBr), ν (cm^{-1}): 3 083, 1 630, 1 540 and 1 380. GC-MS: observed 381.0 (M^+); calculated 380.8 ($C_{22}H_{31}NOFe$).

1.6 Preparation of hydrogen-terminated Si(100) wafers

Single side polished (100) oriented silicon wafer (n-Si, ~0.05 Ω·cm resistivity; p-Si, ~0.02 Ω·cm resistivity) with an area of ca. 2.25 cm^2 was boiled in 3:1 (*V*/*V*) concentrated H_2SO_4/30% H_2O_2 for 30 min (Notice: piranha solution reacts violently with organic materials and should be handled with extreme care), and rinsed copiously with Milli-Q water (18 MΩ). Then they were etched with 10% aqueous HF for 10 min,

rinsed with water again, dried under a stream of N_2 and immediately used in the next functionalisation process.

1.7 Preparation of Ferrocene-Terminated surfaces

Formation of monolayers by attachment of alkenes was achieved using a method of microwave irradiation at a frequency of 2 450 MHz. Hexadecane was melted to prepare the 2.5% (*w*/*w*) FcUA solution, and then deoxygenated by nitrogen for 1 h. The freshly prepared H-terminated Si(100) wafers were put into 2 mL FcUA solution and kept under a nitrogen atmosphere for 1 h. The microwave irradiation power was 200 W and the reactions were conducted in a glass vessel for 15 min under nitrogen atmosphere. After irradiation, the sample was taken out, and subjected to a cleaning procedure consisting of two washing cycles (one cycle involves rinsing by $CHCl_3$ 5 min, and CH_3CN 5 min), and finally dried in a stream of N_2.

1.8 Electrochemistry

An ohmic contact was made to the back of the derivatized silicon wafer by scratching and rubbing the Si surface with the Ga-In eutectic, finally a copper wire was connected on the Ga-In eutectic. The electrode set-up was obtained by pressing the Si crystal against an O-ring as sealing for a small vessel in the PTFE cell. The O-ring defined exactly the electrode area (1.33 cm^2). The electrochemical properties of the Fc-terminated monolayers on silicon were explored by cyclic voltammograms in 0.1 $mol \cdot L^{-1}$ NEt_4ClO_4 solution of dry THF. Electrochemical experiments were performed on an Autolab PGSTAT-30 digital potentiostat/galvanostat (Eco Chemie BV, Utrecht, Netherlands) in a conventional three-electrode system. The counter electrode was a platinum coil, and an Ag/Ag^+ reference electrode.

1.9 XPS

XPS (VG, ESCALB MK-Ⅱ) with a monochromatized Mg $K\alpha$ X-ray source (300 W) was employed to analyze the monolayers on silicon surfaces. The silicon sample with a diameter of 1.0 cm was embedded in a Ni substrate with double glue. Survey scans (CAE=0 eV, step=0.50 eV) over a binding energy 0~1 150 eV were used to obtain the elemental information, and the followed high-resolution scans of Fe2*p*, C1*s*, O1*s*, N1*s*, and Si2*p* photoelectron (CAE=20 eV, step=0.05 eV) to quantitatively determine binding energies and atomic concentrations. All binding energies were normalized to C1*s* at 285.0 eV. Measurements were carried out with a take-off angle of 45 degrees with respect to the sample surface. Peak-fitting was done by using the ESCALB MK-Ⅱ software.

1.10 IR

IR spectra were recorded on a Bruker IFS66/S instrument at 4 cm^{-1} resolution. Grazing angle external reflection accessory with incident angle of 80° and p-polarized light was used. Detection was accomplished by placing a gold mirror behind the silicon wafer. The spacer distance between mirror and silicon is 1 mm, and the detector used for measurement is DTGS. Double-side-polished (111) oriented p-type silicon wafers (B doped, ~15 Ω·cm resistivity and 0.5 mm thick) were cut into rectangular shapes (2×2 cm^2) for IR analysis.

1.11 CSAFM

All operations were carried out on a Multimode SPM with the PicroSPM Ⅱ controller (Molecular Imaging, Temp, AZ). AFM imaging was done under ambient conditions (with a relative humidity of 20% at 26 ℃) using a contact mode AFM with Pt-coated commercial Si_3N_4 cantilevers (MikroMasch USA). The experimental error is dominated primarily by the uncertainty in the exact number of molecules forming the junction. Because the tip drifted over the surface, variations in the number of contacting molecules might cause fluctuation in the measured current. In addition, variations in the chemical environment across the monolayer surface could also introduce experimental error in measurement. This allows us to program the voltage applied to the sample and to collect data continuously while the bias sweeps. To avoid from the breakdown of the FcUA monolayer on silicon surface, the positive and negative branches of the current-voltage curve were obtained by scanning the bias from 0 V to −10 V or 0 to +10 V, respectively. The probe must stay over the same location to within a small fraction of a nanometer during data acquisition to avoid

artifacts associated with instrumental drift.

The current flowed across the monolayer in response to changes of bias voltage was measured when the tip approached stepwise towards the silicon surface. Before the tip contacted the molecules in the monolayer, essentially no current in excess of the noise (~0.3 pA) flowed. When a current greater than the noise level was observed, the first and some subsequent *I-V* curves were recorded, which were taken at different locations on the same sample, and with samples of different batches. As these experiments were performed under ambient conditions, some infrequent and random features were associated with a variety of spurious perturbative effects, such as the random passing of transient contaminants under or on the tip, or stochastic changes in the electronic structure of an unstable tip (e.g. random noise)[24,50]. To avoid the uncertainties caused by the tip scratching and get stable and reproducible *I-V* relations, the current signal was recorded as follows. Since the humidity of the environment had an influence on the current signal, a stream of N_2 blew the chamber until the humidity reached 20%. After the tip stress was increased to a certain value to meet the tip contact with the sample surface, the current signal was recorded. To study the electron transfer of FcUA-Si(100) in detail, the *I-V* measurement on both highly doped n-Si and p-Si was carried out.

2　Results and discussion

2.1　Characterization of the FcUA monolayer on Si(100) by XPS, IR and AFM

XPS is used to analyze the elements presented on the surface, their surface concentrations, and their chemical shifts. The Fc-modified Si(100) surface was examined. Fig.1a is the XPS survey spectra and Table 1 lists the elemental concentrations of the sample. Obviously Fe2*p*, N1*s*, O1*s*, C1*s*, and Si2*p* are the main peaks in the surface. First Fe and N are two characteristic elements on the surface and their atomic ratios (Fe/N, C/N, and C/Fe), deduced from relative peak intensities, are almost equal to the ideal FcUA stoichiometry.

Fig.1b~f show the evolution of the high-resolution XPS spectra of Fe2*p*, C1*s*, N1*s*, O1*s*, and Si2*p*. The $Fe2p_{3/2}$ and $Fe2p_{1/2}$ peaks, clearly visible in Fig.1b at 711.3 and 724.0 eV, respectively , are consistent with Fc groups in the literature[43]. The peak of N1*s* appears at 400.4 eV in Fig.1d, in accordance with our previous statement that organic nitrogen functionalities normally give N1*s* binding energies in the narrow region 399~402 eV[44]. The binding energies of O1*s* from

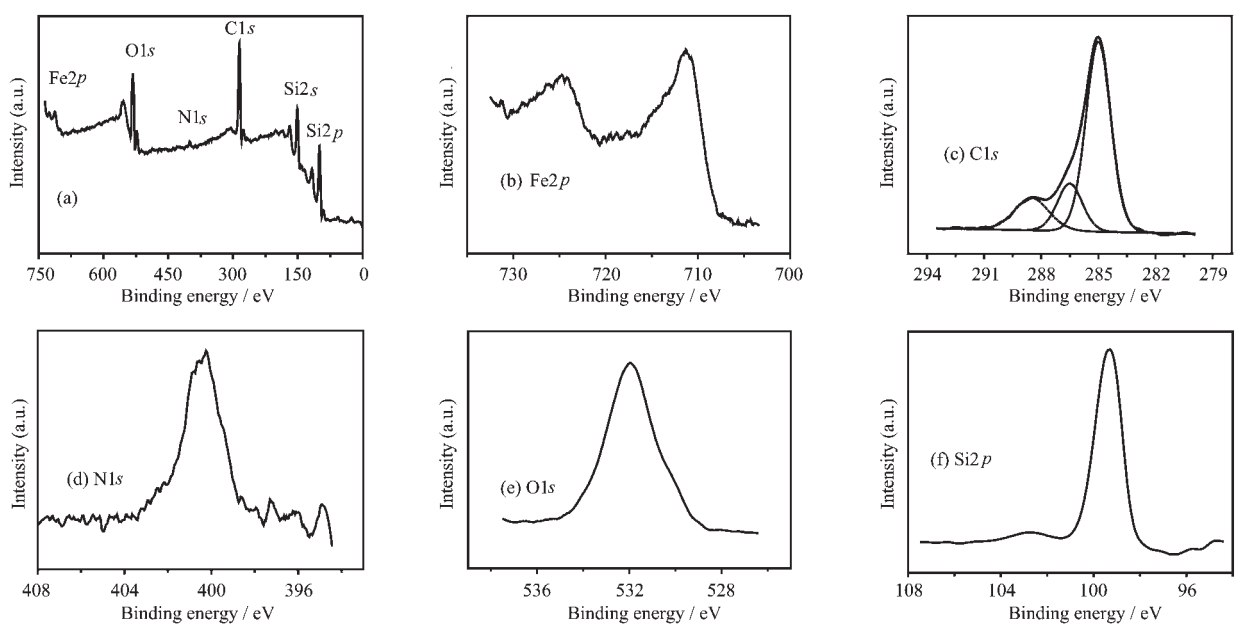

Fig.1　XPS spectra from FcUA-Si(100) surface: (a) full, (b) Fe2*p*, (c) C1*s*, (d) N1*s*, (e) O1*s* and (f) Si2*p*

Table 1 Atomic ratios of elements Fe, C, N, O and Si, and the deconvolution of C1*s* for FcUA-Si(100)

Element(orbital)	E_b / eV	Assignment	Atomic ratios (/C) / %	
			Found	Calcd.
C1*s*	285	alkyl C-C, C=C	1.000	1.000
	286.5	C-N		
	288.5	C(O)-NH		
O1*s*	532	Si(O), C=O	0.139	
Si2*p*	99.3	Si-Si, Si-C	0.136	
	102.7	Si-O-Si		
N1*s*	400.3	C(O)-NH	0.049	0.045
Fe2*p*	711.3	$Fe2p_{3/2}$	0.046	0.045
	724	$Fe2p_{1/2}$		

most organic functionalities fall within a narrow range of ~2 eV around 532.5 eV. Fig.1e shows O1*s* at 532.3 eV, attributable to C=O and oxidized silicon species. In Fig.1f, the peak of Si2*p* at 99.3 eV is attributed to the signal of silicon metal (Si)Si2*p*. Another very small peak at 102.7 eV is attributed to silicon oxide (O) Si2*p*, which shows only a tiny amount of oxide development on the surface. The C1*s* of alkyl carbon is at 285.0 eV and that of aryl carbon at 284.5 eV. Oxygen and nitrogen bound to carbon induce shifts of C1*s* to higher binding energy by 1.5 eV per C-O (or C-N) bond. And C1*s* of carbonyl carbon C=O in aldehyde, ketone, and amide is 288.5 eV. In Fig.1c, C1*s* can be deconvoluted into three peaks, a main peak centered at 285.0 eV due to hydrocarbon CH_2 containing both covalently bound and physisorbed carbons, and two weak peaks at 286.5 and at 288.5 eV due to C-N and amide-C atoms in FcUA. By the data of XPS, one could conclude that the FcUA monolayer on Si(100) has been prepared by Si-C bonds.

In our work, microwave irradiation was used to initiate the reaction between Si-H and C=C on the flat silicon surface[45,46]. Does the microwave irradiation destroy the molecular structure of FcUA? The IR spectrum of the FcUA monolayer prepared under the identical reaction conditions shown in Fig.2 will answer this question. The strong hydrocarbon bands are easily detected at 2 927 and 2 855 cm^{-1}, known to the asymmetric and symmetric stretching vibrations of C-H_2. Characteristic amide Ⅰ and amide Ⅱ bands appear at 1 637 and 1 545 cm^{-1}. Therefore primary chemical

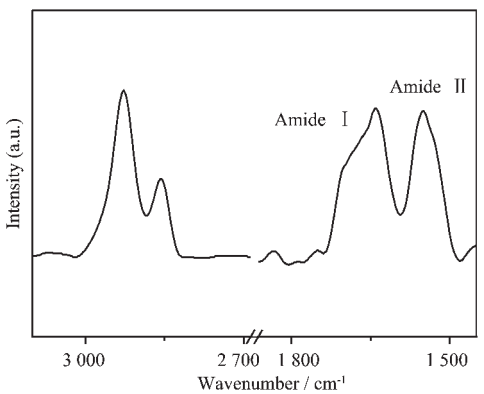

Fig.2 IR spectrum of FcUA-Si(100) sample

structures (-$(CH_2)_9$- and -NH-C(O)-) of FcUA are retained after microwave irradiation. The spectrum of the FcUA monolayer on Si(100) indicates that the Fc moiety is intacted after FcUA molecules are grafted on the silicon surface. Both IR and XPS indicates that the microwave irridiation is more effective and simpler than thermal heating and UV irradiation[19,20].

AFM images taken on freshly prepared H-terminated Si(100) sample (Fig.3a) and their associated linear cross-section profiles show that the surface is flat in view of the field (1 100×1 100 nm^2). The topography varies in the range of 0.1~0.2 nm; the corrugation along the white line in the image is reported in Fig.3a. Fig.3b (1 100×1 100 nm^2) shows a similar set of data, image and profiles of FcUA monolayer as in Fig.3a. However, the corrugation changes appreciably with respect to the bare substrate, giving rise to topographical variations of 0.05~0.1 nm. The observed flatness is of the same magnitude as reported recently by Sun

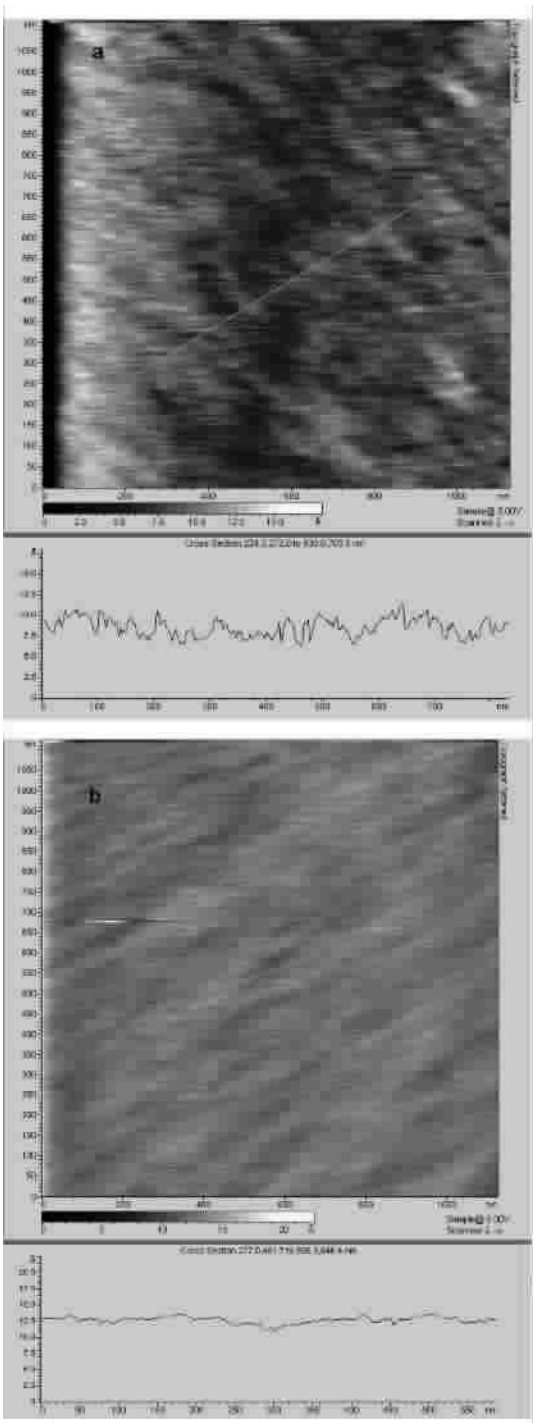

Fig. 3　(a) AFM image (1 100×1 100 nm^2) in a top-view representation from Si(100)-H, (b) AFM image (1 100×1 100 nm^2) in a top-view representation from FcUA-Si(100)

et al. for the *n*-hexadecyl-modified Si(100)[47]. In addition, Condorelli et al. used AFM to study 10-undecenoate-modified Si(100) and reported a roughness of less than 0.1nm[48]. These studies are consistent with the hypothesis of a single molecular monolayer covalently bonded to the substrate. So from our results, we can confirm a homogeneous monolayer grafted onto silicon (100) surface.

2.2　Amount of FcUA molecules and the stability of the FcUA monolayer on Si(100) by electrochemical studies

Representative cyclic voltamograms for FcUA-Si (100) are shown in Fig.4a and the FcUA monolayer exhibits robust and reversible redox behavior. A control experiment was carried out on the bare p-Si(100) without FcUA and its CV curves did not show any reversible redox behavior. The electrolyte solution contained no deliberately added electroactive species, therefore the volt metric peaks are unambiguously attributed to the attached redox species ($Fc^{II} \rightleftharpoons Fc^{III}$)[19,20]. The CV curves vs scan rates were further analyzed. As can be inferred from inspection of Fig.4b, the anodic peak currents are found to scale linearly with the scan rate v rather than with $v^{1/2}$, which indicates a surface-

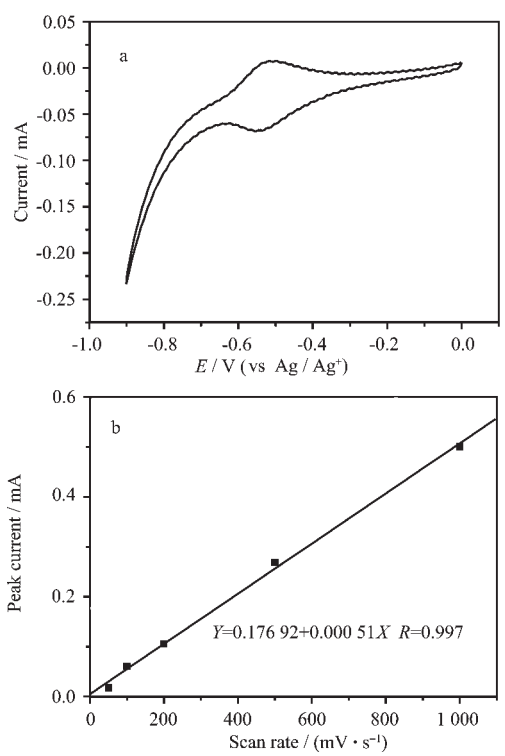

Fig.4　(a) Cyclic voltammograms of a FcUA-Si(100) electrode in 0.1 mol·L^{-1} NEt_4ClO_4 in dry THF, as a function of potential scan rate 1 V·s^{-1}. (b) Anodic peak current as a function of cyclic voltammograms scan rate, with correlation coefficients of 0.997

confined process. The surface coverage of the covalently attached molecules can be determined by using the equation (**1**)[49].

$$I_{peak} = n^2FvA^2\Gamma(4RT)^{-1} \quad (\mathbf{1})$$

where n is the number of electrons, F is the Faraday constant, v is the scan rate ($V \cdot s^{-1}$), A is the electrode surface area (cm^2), Γ is the surface coverage in moles of attached molecules per unit surface area (cm^2), R and T have their usual meanings. The surface coverage (Γ) value is 2.3×10^{13} cm^{-2} for the FcUA monolayer. According to the optimal stacking distance as obtained by a PM3 calculation[23], the Fc experimental coverage is more than 1/10 of the closest 2D packing (The calculated value is 2.0×10^{14} cm^{-2}). The AFM images and the data of CV show that a homogeneous but not tight monolayer is assembled by FcUA molecules on the silicon surface.

Under ambient conditions, the voltammetric characteristics of the FcUA monolayer are stable over repeated cycling through hundreds of scans. A relatively increasing ratio (480.9%) of SiO_2/Si(Si, C) can be clearly seen from the data in Table 2, which is caused by oxidation during electrochemistry measurement. Relative with the changes of SiO_2/Si (Si, C), the reduction of the Fe/Si_{total} (36.2%) and N/Si_{total} ratio (39.4%) due to the tiny surface detachment of FcUA molecules had also been observed[19,20], which show that FcUA monolayers stay robust on the silicon surface.

2.3 The electron transfer of the FcUA monolayer on Si (100) by current-voltage (*I-V*) measurement

Table 2 XPS results for FcUA-Si(100) before and after CV measurements

Sample	Atomic ratios / %			
	SiO_2 / Si	Fe / Si_{total}	N / Si_{total}	C / Si_{total}
Before CV	4.2	24.3	28.7	735.2
After CV	24.4	15.5	17.4	948.1

Their typical *I-V* curves are chosen and shown in Fig.5. The reverse threshold voltage, V_T, is defined as the value of the intercept between a linear extrapolation of the exponential tails and the zero-current axis. Fig.5a and 5b show two typical *I-V* curves taken on the bare p-Si-H and n-Si-H surfaces. In Fig.5a, a typical diode-like behavior is observed. Relative to the Pt tip, the positive branch is forward and the negative branch is reverse and V_T in the negative bias direction is~−1.2 V. But in Fig.5b, an opposite diode-like behavior appears and its V_T is~+3.9 V. The origin of the diode-like behavior can be attributed to the work function difference between Pt and p- or n- silicon substrate.

Comparing Fig.5c with 5a, V_T increases from ~ −1.2 V to~−4.8 V after grafting FcUA monlayer. And for n-Si (Fig.5d and 5b), V_T also increases form ~ +3.9 V to ~ +6.2 V. Despite of the silicon types, all V_T increases after FcUA attachment. The excess V_T of FcUA-Si relative to the bare Si is due to FcUA monolayer. According to the molecular height of FcUA (~2.4 nm), its dielectrical strength is calculated as high as 1.5 $GV \cdot m^{-1}$ on p-Si (or 1 $GV \cdot m^{-1}$ on n-Si). Considering the coverage and the orientation of FcUA molecule on the silicon surface [18], the value of its dielectrical strength is slightly lower than that of the pure long chain alkyl monolayer (2.0 $GV \cdot m^{-1}$)[4,5].

At the positive branch of Fig.5c, currents fluctuate beginning at ~+1.0V, relative to the *I-V* curve of the bare p-Si in Fig.5a. Smoothing of the data in Fig. 5c through adjacent point averaging leads to the NDR-like peak at +1.8 V. It occurs frequently in the range of +1.0~2.0 V, which is in accordance with the

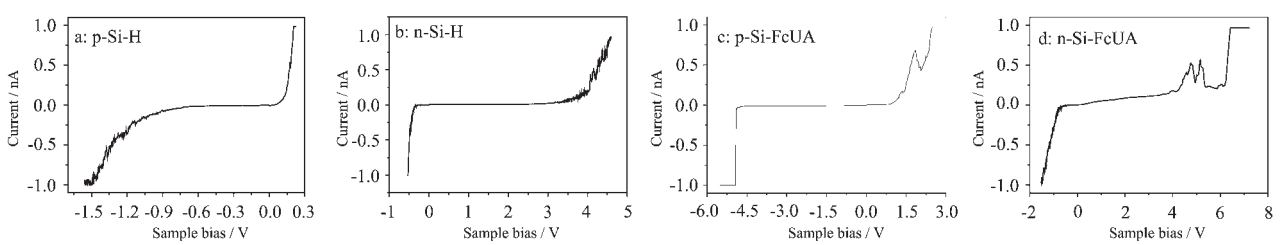

Fig.5 Typical *I-V* curves of (a) p-Si-H, (b) n-Si-H, (c) p-Si-FcUA and (d) n-Si-FcUA. The positive and negative branches of the *I-V* curve were obtained by scanning the bias from zero in the positive and negative directions, respectively

NDR peak (1.5±0.3 V) of Fc-terminated monolayer on gold[24~27]. In Fig.5d, there are also multiple peaks detected at ~ +5.0 V and they are frequently observed in the range of +4.0 ~6.0 V. In our experiment, it should be noted that the size and width of these peaks are irreproducible and mobile within this bias range.

Another noted phenomenon is that the peaks would diminish and V_T is increased after 3 cycles (Fig.6). Though neutral Fc is quite stable in normal electrolyte, the Fc^+ may undergo degradation by oxidation[51]. With the oxidation of Fc^+ and elimination of the charged species, the degraded products add the Schottky barrier to hinder the charge transfer between the tip and the monolayer [52]. This means that the breakdown of FcUA monolayer is mainly due to the FcUA molecular oxidation and degradation. According to the above results and discussion, these NDR-like peaks are due to the FcUA molecules on the silicon surface. From our experiments, we can rule out the resonant tunneling mechanism that would result in reproducible and stable NDR peaks. Because the NDR-like peaks generally associate with the breakdown of the monolayer in our experiments, we prefer to attribute the mechanism to the FcUA molecular oxidation, decomposition, or even desorption proposed by Wolkow et al[23]. With increasing in the sample bias, the breakdown should be further due to the Fc decomposition (>4.0 V).

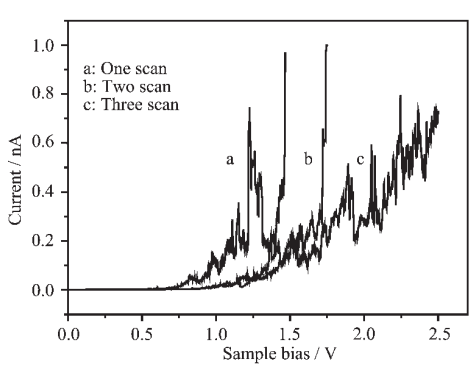

Fig.6　A representative mutli-scaning *I-V* curves of FcUA monolayer on p-Si from zero to positive bias

3　Conclusions

In summary, we synthesized a new electroactive compound (FcUA), and then attached it on Si(100) surface by a simple method of microwave irradiation. The data of XPS, IR, and AFM images indicate a homogeneous monolayer of FcUA on the surface. The reversible redox behavior of FcUA-Si(100) in electrolyte was also proved that Fc was successfully grafted onto the surface. The surface coverage of the FcUA monolayer was calculated to be 2.3×10^{13} cm^{-2}. Finally *I-V* curves of the Pt/FcUA/Si junction were recorded by CSAFM at room temperature. The FcUA monolayer can improve the dielectric strength against the Pt/Si junction. No matter it is n-Si or p-Si, NDR-like peaks are all observed at the positive bias after the FcUA attachment. These peaks should be due to the tuning of FcUA molecules among the Pt/FcUA/Si junctions. We prefer to suggest that these peaks are caused by the FcUA oxidation, decomposition, or even desorption.

References:

[1] Clausen C, Gryko D T, Yasseri A A, et al. *J. Org. Chem.*, **2000**,**65**:7371~7378

[2] Roth K M, Dontha N, Dabke R B, et al. *J. Vac. Sci. Tchonl. B.*, **2000**,**18**:2359~2364

[3] Lenfant S, Kreminski C, Delerue C, et al. *Nano. Lett.*, **2003**, **3**:741~746

[4] Zhao J W, Uoski K. *J. Phys. Chem. B.*, **2004**,**108**:17129~17135

[5] Barrelet C J, Bobinson D B, Cheng J, et al. *Langmuir*, **2001**, **17**:3460~3465

[6] Haber J A, Lauermann I, Michalak D, et al. *J. Phys. Chem. B.*, **2000**,**104**:9947~9950

[7] Cheng J, Bobinson D B, Cicero R L, et al. *J. Phys. Chem.* B., **2001**,**105**:10900~10904

[8] Liu Y J, Yu H Z. *Chem. Phys. Chem.*, **2002**,**3**:799~802

[9] Wang W, Lee T, Kamdar M, et al. *Superlattices Microstruct.*, **2003**,**33**:217~226

[10]Wei L Y, Syomin D, Loewe R S, et al. *J. Phys. Chem. B.*, **2005**,**109**:6323~6330

[11]Yasseri A A, Syomin D, Loewe R S, et al. *J. Am. Chem. Soc.*, **2004**,**126**:15603~15612

[12]Rappich J, Merson A, Roodenko K, et al. *J. Phys. Chem. B.*, **2006**,**110**:1332~1337

[13]Cleland G, Horrocks B R, Houlton A. *J. Chem. Soc. Faraday Trans.*, **1995**,**91**:4001~4003

[14]Eagling R. D, Bateman J E, Goodwin N J, et al. *J. Chem. Soc. Dalton Trans*., **1998**,1273~1275

[15]Houlton A, Horrocks B R, Gibson A E, et al. *J. Chem. Soc. Dalton Trans*., **1999**,3229-3234.

[16]Roth K M, Yasseri A A, Liu Z, et al. *J. Am. Chem. Soc*., **2003**,**125**:505~517

[17]Buriak J M. *Chem. Rev*., **2002**,**102**:1271~1308

[18]Wayner D D M, Wolkow R A. *J. Chem. Soc., Perkin Trans*., **2002**,**2**:23~34

[19]Dalchiele E A, Aurora A, Bernardini G, et al. *J. Electroanal. Chem*., **2005**,**579**:133~142

[20]Zanoni R, Cattaruzza F, Coluzza C, et al. *Surf. Sci*., **2005**, **575**:260~272

[21]Kruse P, Johnson E R, Dilabio G A, et al. *Nano. Lett*., **2002**, **2**:807~810

[22]Gorman C B, Carroll R T, Fuierer R R. *Langmuir*, **2001**,**17**: 6923~6930

[23]Wassel R A, Credo G M, Fuierer R R, et al. *J. Am. Chem. Soc*., **2004**,**126**:295~300

[24]Tivanski A. V, Walker G C. *J. Am. Chem. Soc*., **2005**,**127**: 7647~7653

[25]He J, Lindsay S M. *J. Am. Chem. Soc*., **2005**,**127**:11932~ 11933

[26]Wold D J, Frisbie C D. *J. Am. Chem. Soc*., **2001**,**123**:5549~ 5556

[27]Ramachandran G K, Hopson T J, Rawlett A M, et al. *Science*, **2003**,**300**:1413~1416

[28]Beebe J M, Engelkes V B, Miller L L, et al. *J. Am. Chem. Soc*., **2002**,**124**:11268~11269

[29]Wold D J, Frisbie C D. *J. Am. Chem. Soc*., **2000**,**122**:2970~2971

[30]Fan F R, Lai R Y, Cornil J, et al. *J. Am. Chem. Soc*., **2004**, **126**:2568~2573

[31]Xiao X Y, Nagahara L A, Rawlett A M, et al. *J. Am. Chem. Soc*., **2005**,**127**:9235~9240

[32]Rawlett A M, Hopson T J, Nagahara L A, et al. *Appl. Phys. Lett*., **2002**,**81**:3043~3045

[33]Kuznetsov A M, Sommer-Larsen P, Ulstrup J. *Surf. Sci*., **1992**,**275**:52~64

[34]Mazur U, Hipps K W. *J. Phys. Chem*., **1995**,**99**:6684~6688

[35]Guisinger N P, Greene M E, Basu R, et al. *Nano. Lett*., **2004**,**4**:55~59

[36]Guisinger N P, Greene M E, Basu R, et al. *Nanotechnology*, **2004**,**15**:S452~S458

[37]Rakshit T, Liang G C, Ghosh A W, et al. *J. Comput. Electron*., **2005**,**4**:83~86

[38]Rakshit T, Liang G C, Ghosh A W, et al. *Phys. Rev. B*., **2005**,**72**:125305~1~125305~8

[39]Rakshit T, Liang G C, Ghosh A W, et al. *Nano. Lett*., **2004**, **4**:1803~1807

[40]Pitters J L, Wolkow R A. *Nano. Lett*., **2006**,**6**:390~397

[41]BÖcking T, James M, Coster H, et al. *Langmuir*, **2004**,**20**: 9227~9235

[42]Kraatz H B, Lusztyk J, Enright G D. *Inorg. Chem*., **1997**,**36**: 2400~2405

[43]Qi H, Sharma S, Li Z, et al. *J. Am. Chem. Soc*., **2003**,**125**: 15250~15259

[44]Xiao S J, Brunner S, Wieland M. *J. Phys. Chem. B*., **2004**, **108**:16508~16517

[45]Guo D J, Xiao S J, Xia B, et al. *J. Phys. Chem. B*., **2005**,**109**: 20620~20628

[46]Boukherroub R, Petit A, Loupy A, et al. *J. Phys. Chem. B*., **2003**,**107**:13459~13462

[47]Sun Q Y, L. de Smet C. P. M, van Lagen B, et al. *J. Am. Chem. Soc*., **2005**,**127**:2514~2523

[48]Condorelli G G, Motta A, Fragalà I L, et al. *Angew. Chem. Int. Ed*., **2004**,**43**:4081~4084

[49]Finklea H O, in: Meyers R A (Ed.) *Encyclopedia of Analytical Chemistry*, Chichester: John Wiley and Sons Ltd., **2000.**

[50]Chen J, Reed M A, Rawlet A M, et al. *Science*, **1999**,**286**: 1550~1552

[51]Zotti G, Schiavon G, Zecchin S, et al. *J. Electroanal. Chem*., **1998**,**456**:217~221

[52]Selzer Y, Salomon A, Ghabboun J, et al. *Angew. Chem. Int. Ed*., **2002**,**41**:827~830